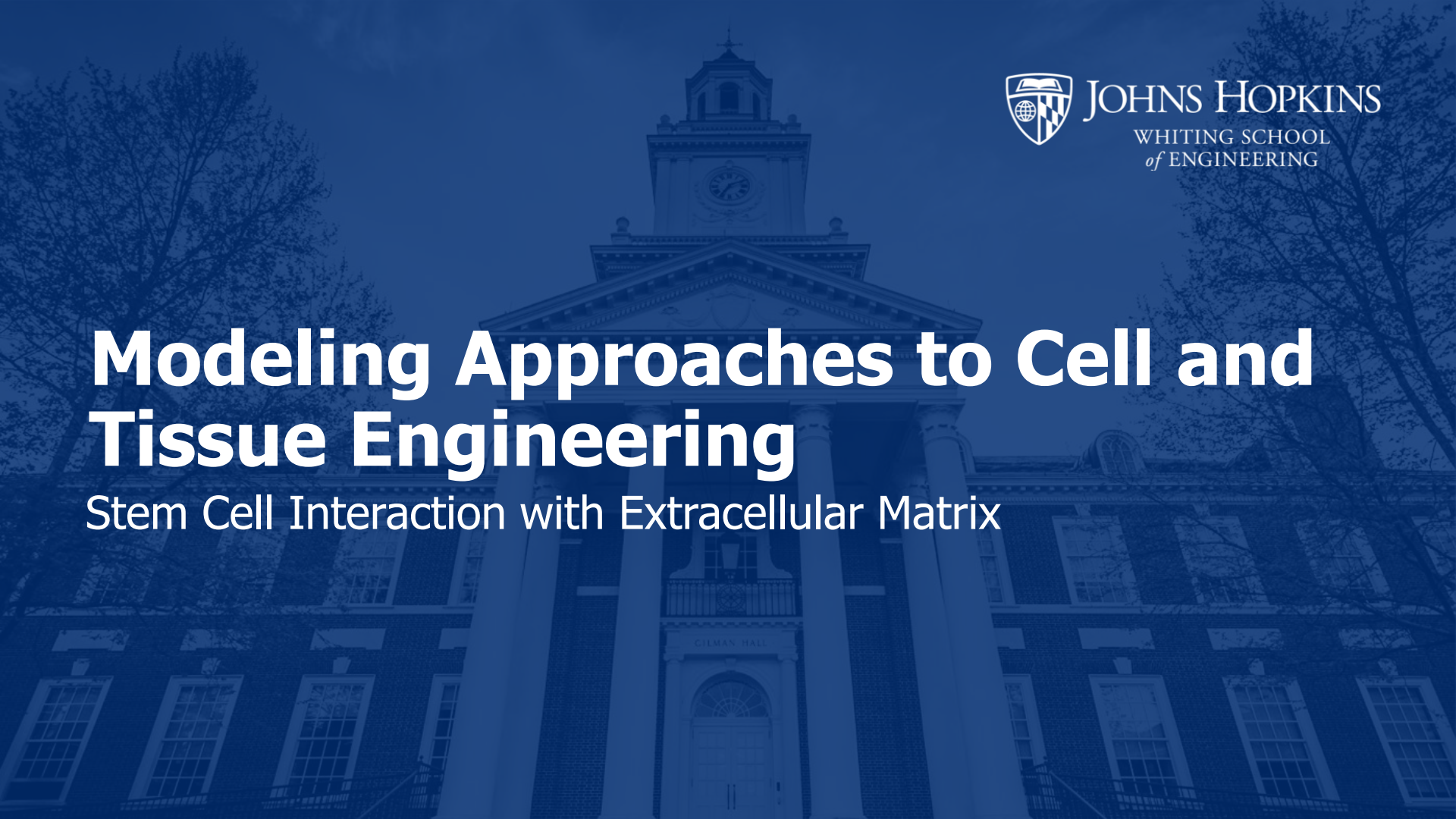

Modeling Approaches to Cell and Tissue Engineering

Stem Cell Interaction with Extracellular Matrix

Overview

Lectures 10, 11, and 13 cover the broad topic of stem cell interaction with ECM. Lectures 10 and 11 deal with the effects of ECM stress relaxation on cell spreading, prolife1ation, and differentiation. Lecture 10 mainly focuses on the phenomenological aspect of the problem, and Lecture 11 uses a Maxwell model to describe the phenomena associated with cell/ECM interaction. **(Alex Spector after Chaudhuri et al. 2016)**

- Modulating the nanoscale architecture of alginate hydrogels to modulate stress relaxation properties independent of initial elastic modulus and matrix degradation to capture the viscoelastic behaviors of living tissues.
- Cell spreading and proliferation for fibroblasts encapsulated within gels are enhanced with faster stress relaxation.
- MSCs undergo osteogenic differentiation and form an interconnected mineralized collagen-1-rich matrix only in rapidly relaxing gels.
- Osteogenic differentiation of MSCs mediated through ECM ligand density, enhanced RGD ligand clustering, and myosin contractility in stiffer hydrogels.
- Hypothesis for how initial elastic modulus and stress relaxation properties of matrix regulate cellular behaviors.

Alginate Hydrogels with Modulated Architecture

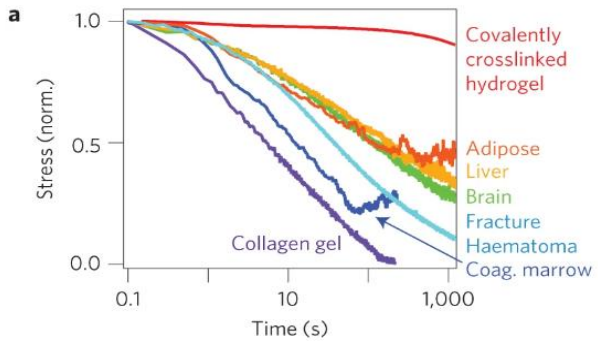

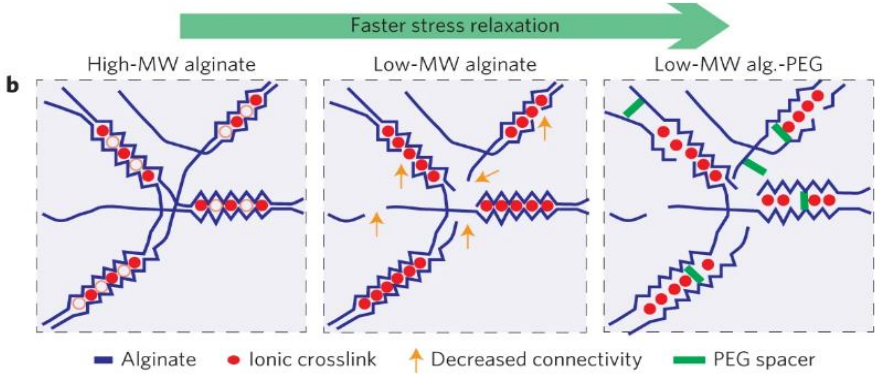

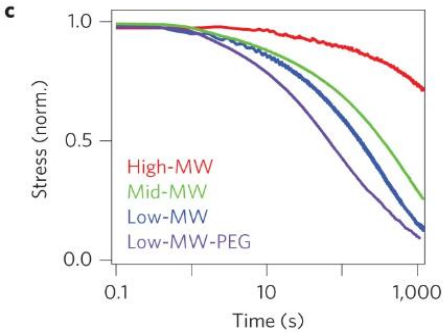

- a, Living tissues are viscoelastic and exhibit stress relaxation. Stress relaxation tests of a crosslinked hydrogel (polyacrylamide), a collagen gel, an initial fracture haematoma (human), and various tissues (rat) at a strain of 15%. Stress is normalized by the initial stress.
- b, Schematic depicting how lowering the molecular weight (MW) of alginate polymers (blue) crosslinked by calcium (red) decreases entanglement and connectivity (orange arrows) of the network, and coupling of small spacers provides a steric spacing of crosslinking zones in the alginate. Both approaches are predicted to increase the rate of stress relaxation.
- c, Stress relaxation tests on gels composed of alginates with different molecular weights, or low-MW alginate coupled to a PEG spacer (15% compressional strain).

Elastic Modulus of the Modulated Hydrogel Changes Insignificantly

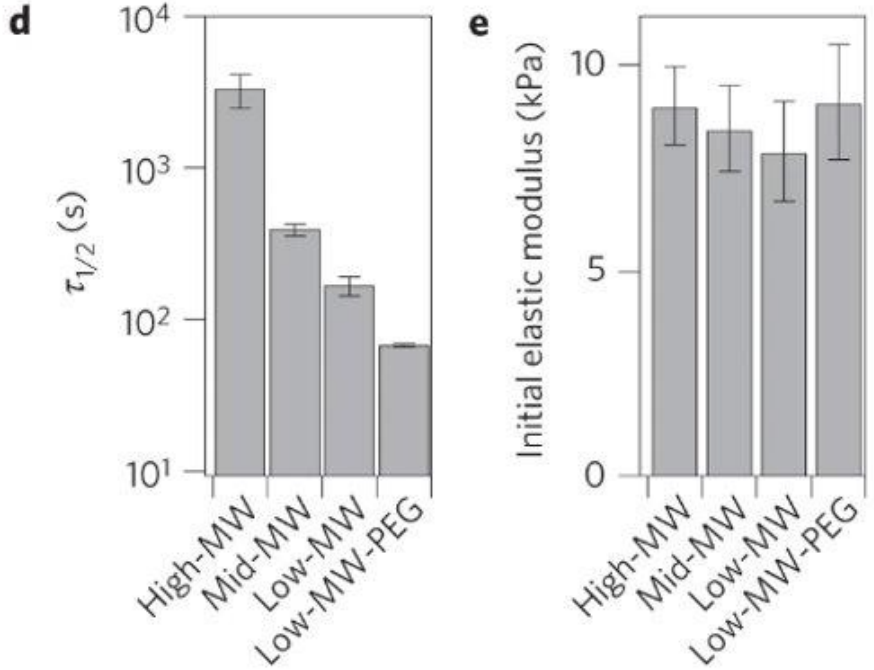

- d, Quantification of timescale at which the stress is relaxed to half its original value, $\tau_{1/2}$, from stress relaxation tests in c. The timescale of stress relaxation decreases significantly with alteration in architecture (Spearman's rank correlation coefficient, $p < 0.0001$).
- e, Initial modulus measurements of gels in c. Differences between elastic moduli are not significant, and elastic moduli show no statistical trend with altered architecture.

Spreading of Cells Encapsulated within Hydrogel

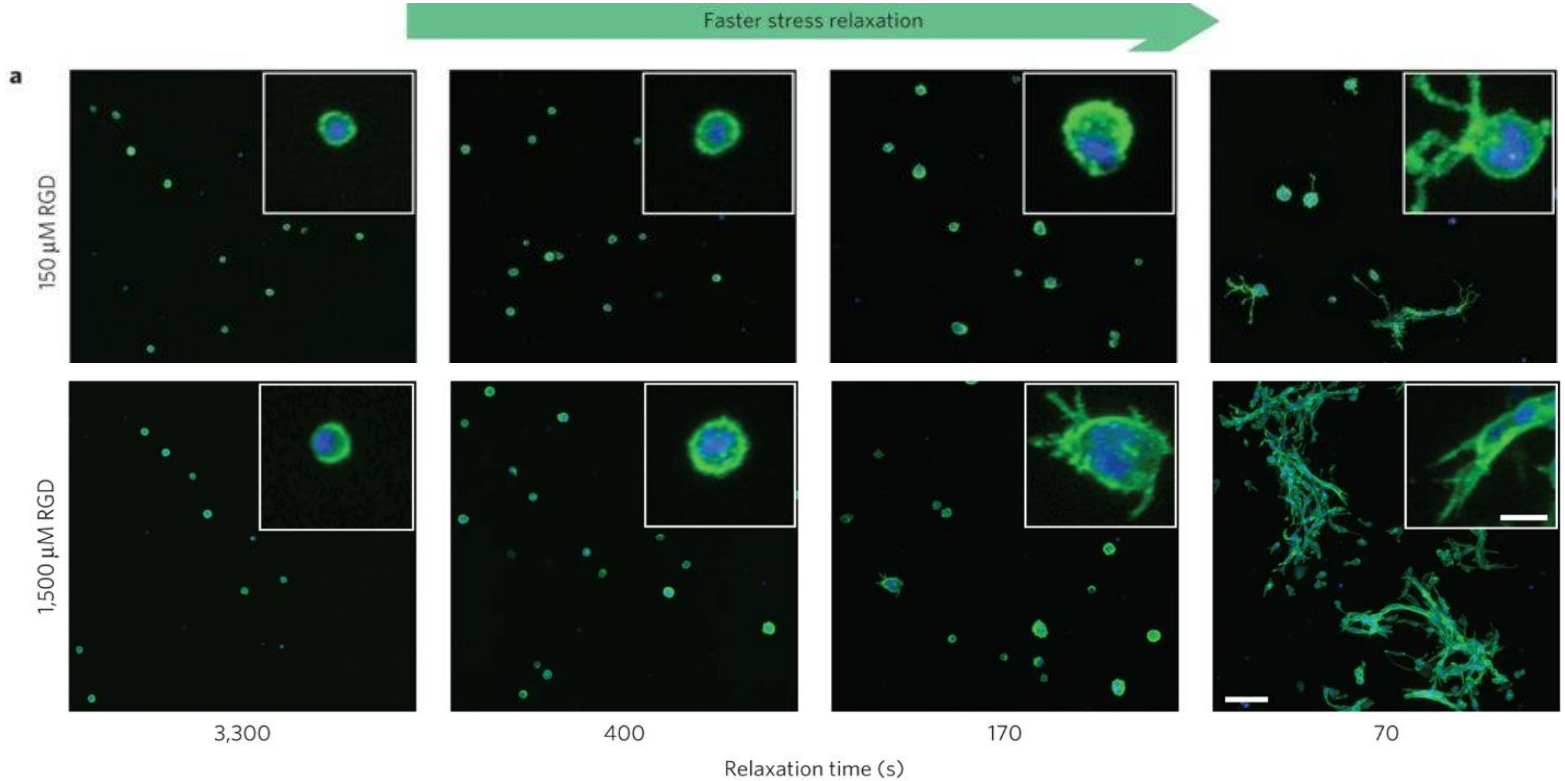

a, Representative images of 3T3 cells encapsulated within alginate gels with the indicated relaxation time $\tau_{1/2}$ for stress relaxation and two RGD concentrations (average initial modulus of 9 kPa). Green colour represents actin staining and blue represents nucleus. Images were taken after seven days in culture. Scale bar is 100 μm for the larger images and 20 μm for the insets.

Spreading and Proliferation Increase Significantly with Faster Stress Relaxation

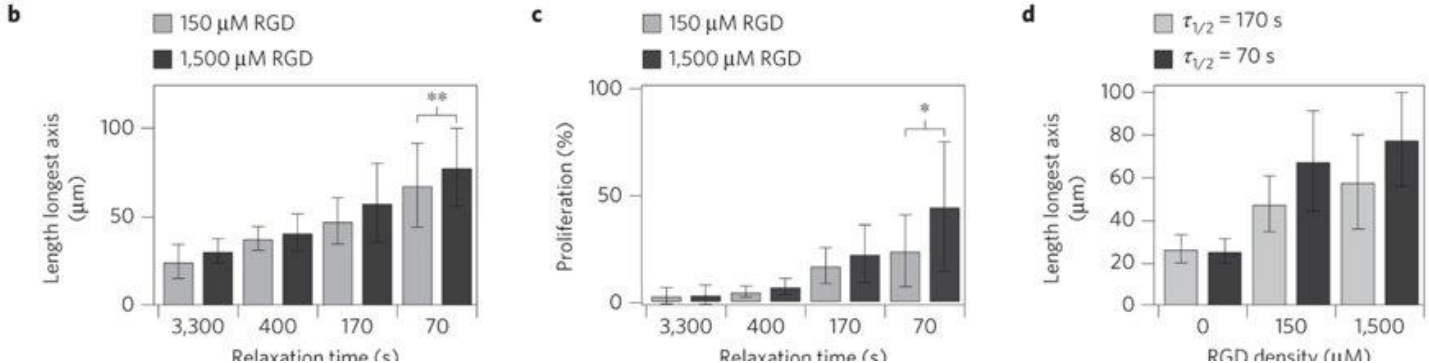

- b, Quantification of the longest dimension of the smallest bounding box fully containing individual 3T3 cells for the indicated conditions. **indicates $p < 0.01$ (Student's *t*-test). Spreading increases significantly with faster stress relaxation (Spearman's rank correlation, $p < 0.0001$ for both values of RGD).
- c, Quantification of proliferating cells. *indicates $p < 0.05$ (Student's *t*-test). Proliferation was found to increase with faster stress relaxation (Spearman's rank correlation, $p < 0.0001$ for both values of RGD).
- d, Quantification of the longest dimension of the smallest bounding box fully containing individual 3T3 cells as a function of RGD density in alginate gels with a relaxation time of 70 or 170 s. Spreading increases significantly with increased RGD concentration for both gels (Spearman's rank correlation, $p < 0.0001$ for both values of $\tau_{1/2}$). Data are shown as mean ± s.d.

Cell Differentiation in Gels of Different Stiffness

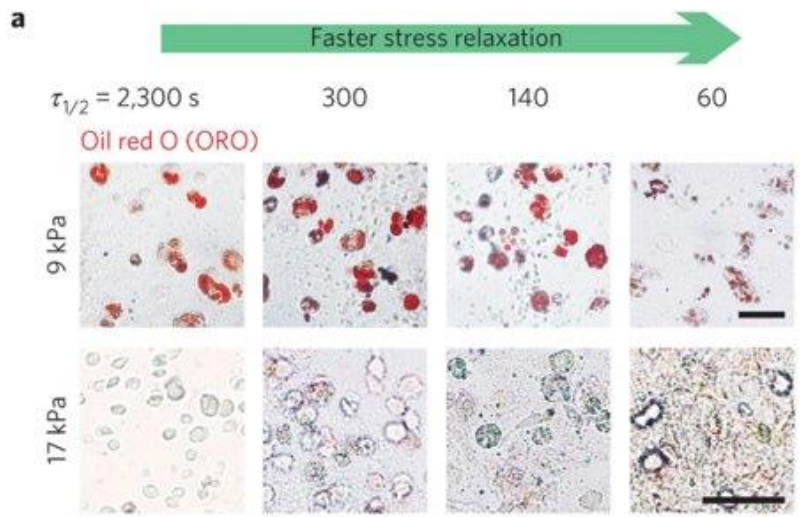

a, Representative images of cryosections with Oil Red O (ORO) staining (red), indicating adipogenic differentiation, and alkaline phosphatase staining (blue), indicating early osteogenic differentiation, for MSC cultured in gels of indicated initial modulus and timescale of stress relaxation for seven days. RGD density is 1,500 μM. Scale bars are 25 μm.

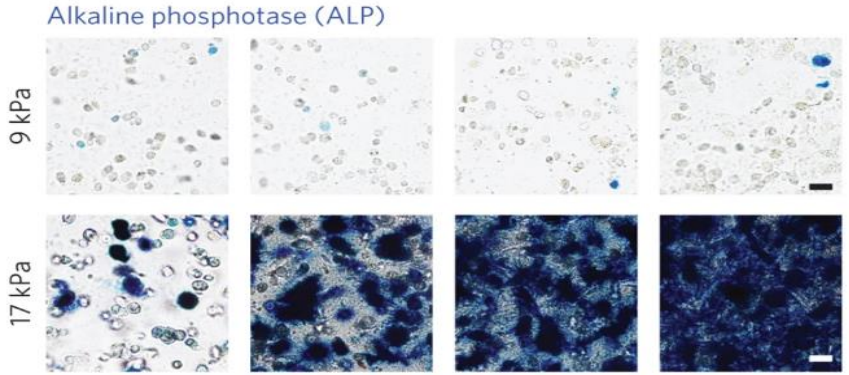

Osteogenic Differentiation Increases Significantly with a Faster Stress Relaxation

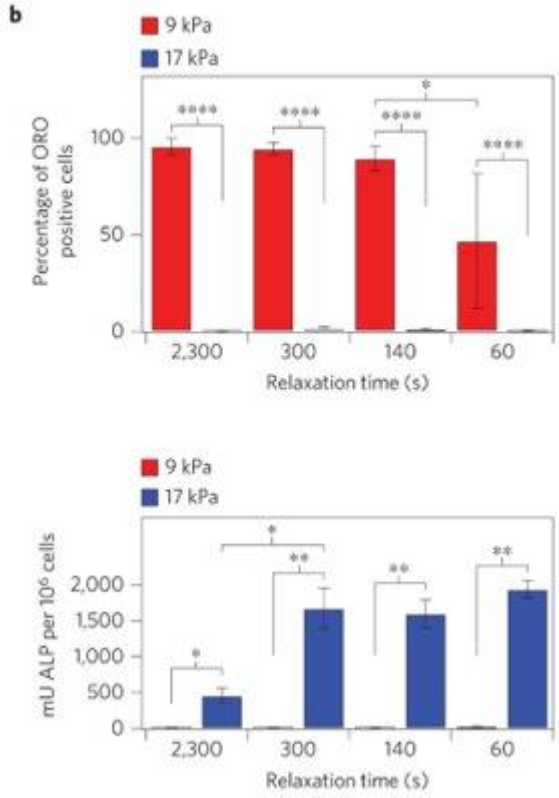

b, Quantification of the percentage of cells staining positive for ORO, and a quantitative assay for alkaline phosphatase activity from lysates of cells in gels from the indicated conditions at seven days in culture. *, **, and ****indicate $p < 0.05$, 0.01, and 0.0001 respectively (Student's *t*-test). Bars for % cells staining for ORO in gels with initial modulus of 17 kPa and alkaline phosphatase activity of cells in gels with initial modulus of 9 kPa are barely visible owing to the small values relative to the other conditions. Osteogenic differentiation increases significantly with a faster stress relaxation (Spearman's rank correlation, $p < 0.0001$).

MSCs/Hydrogel Interaction. Confocal Microscope Images

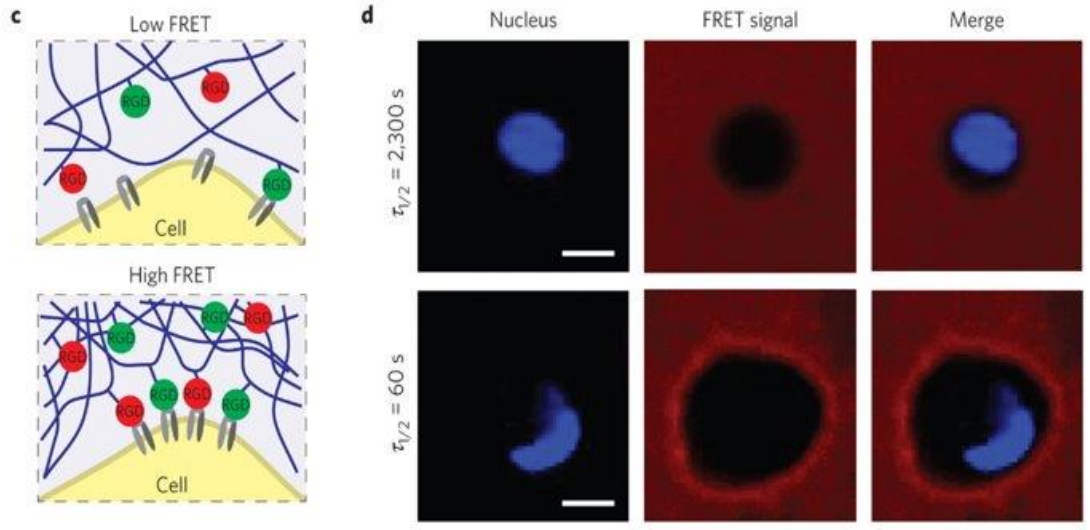

- c, Schematic of assay using FRET between RGD–fluorescein and RGD–rhodamine coupled to different alginate chains to monitor mechanical clustering of RGD ligands at the nanoscale by cells.
- d, Representative confocal microscope images of nucleus (DAPI/blue) and FRET acceptor signal from hydrogel (red) surrounding MSCs cultured in hydrogels with different stress relaxation properties after 18 h of culture. Blank spot in FRET signal images indicates location of cell.

ALP Activity of MSCs

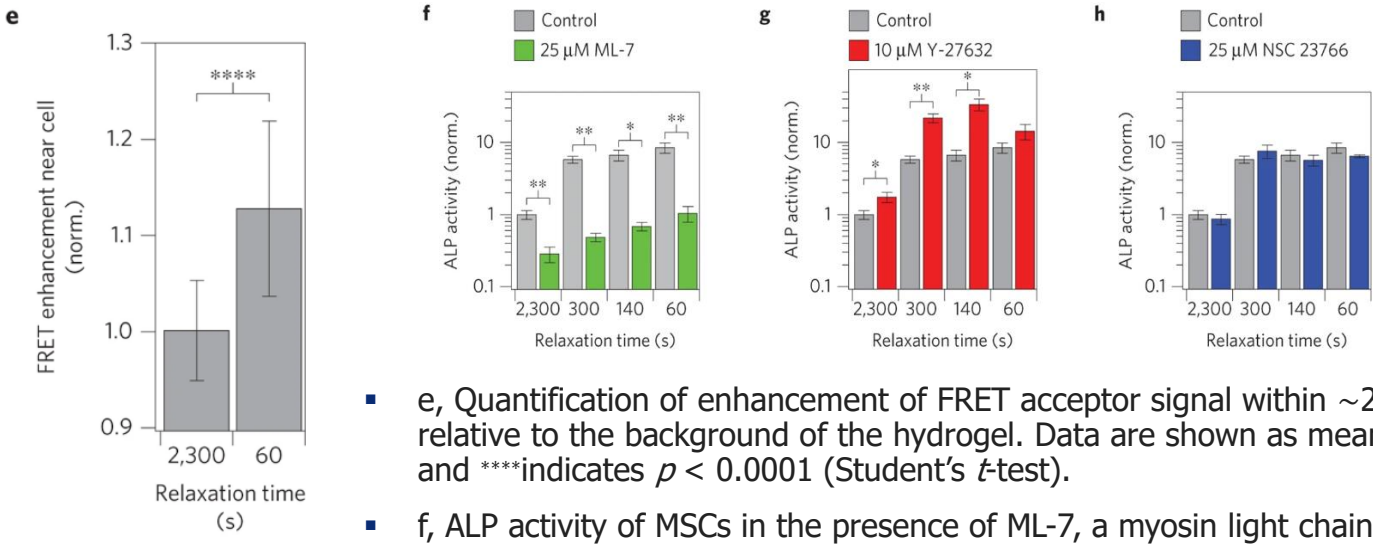

- e, Quantification of enhancement of FRET acceptor signal within ~2–3 μm of cell border relative to the background of the hydrogel. Data are shown as mean ± s.d. and ****indicates $p < 0.0001$ (Student's *t*-test).
- f, ALP activity of MSCs in the presence of ML-7, a myosin light chain kinase inhibitor.
- g, ALP activity of MSCs in the presence of a Rho kinase inhibitor, Y-27632.
- h, ALP activity of MSCs in the presence of a Rac1 inhibitor, NSC 23766. All experiments were done in hydrogels with an initial elastic modulus of 17 kPa and RGD concentration of 1,500 μM. All data are shown as mean ± s.d.*,**indicate $p < 0.05$, 0.01 respectively (Student's *t*-test). Scale bars are all 10 μm.

Images of Actins, Nuclei, and beta1-integrins in MSCs Encapsulated in Hydrogel

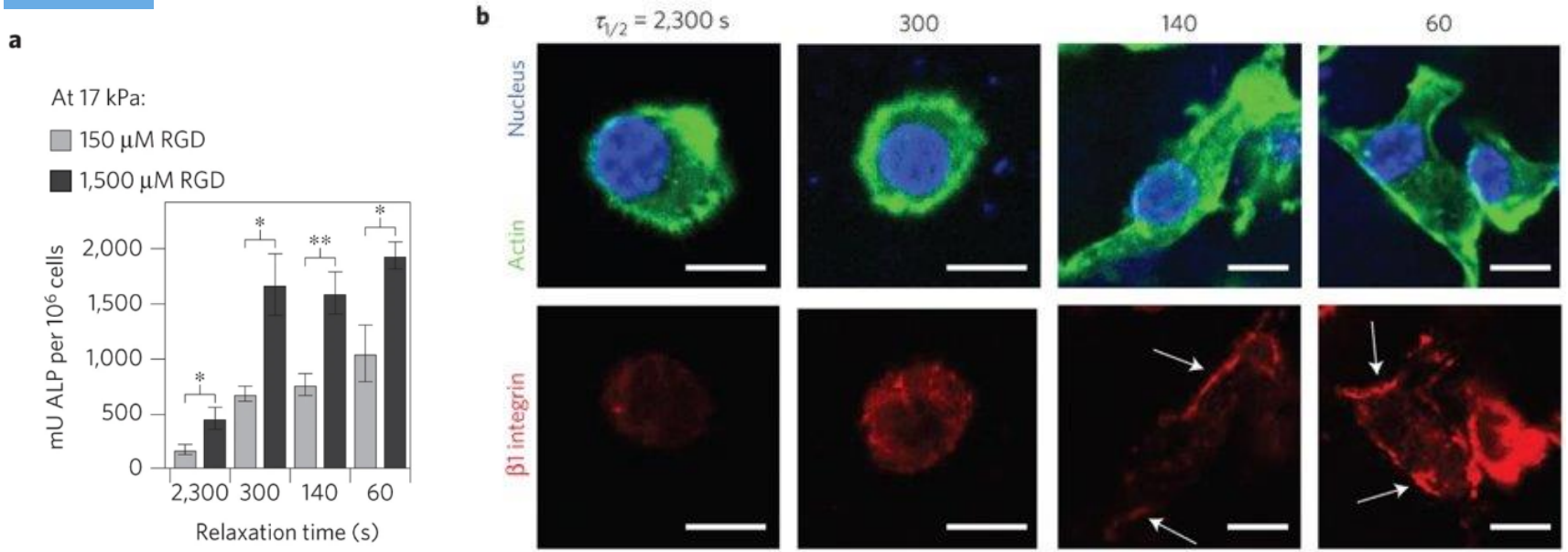

- a, Quantification of ALP activity of MSCs encapsulated in hydrogels with an initial elastic modulus of 17 kPa after seven days in culture with an RGD density of 150 or 1,500 μM.
- b, Representative immunofluorescence staining for actin (green), nucleus (blue) and β1 integrin (red) in MSCs cultured in the indicated conditions for a week.

Cell Interaction with 3-D Viscoelastic Matrix. Stress Relaxation

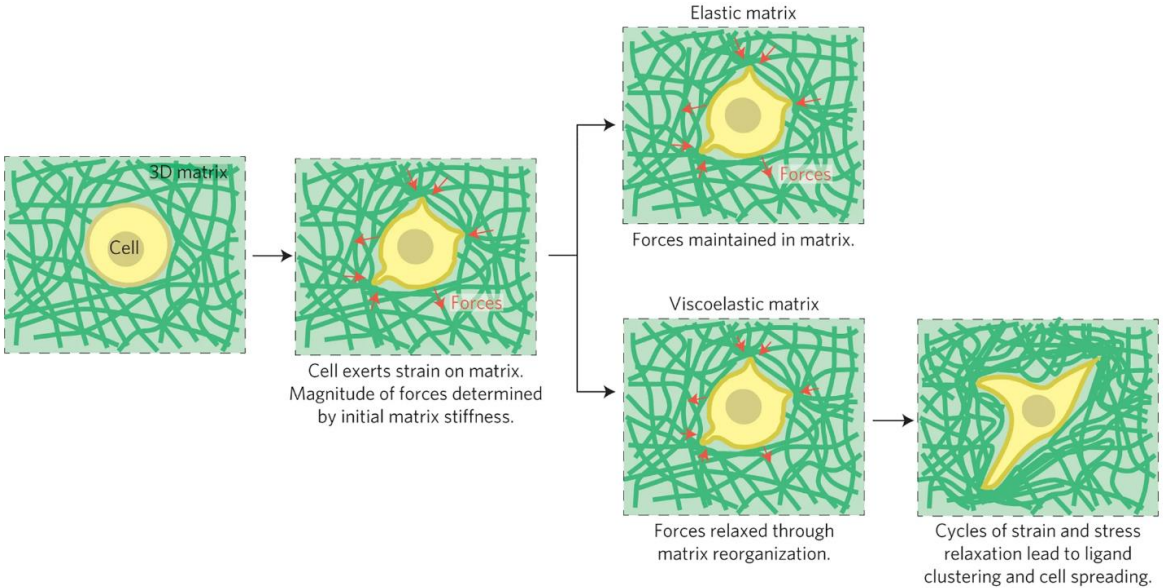

A cell in a 3D matrix initially exerts strains on the matrix, resulting in forces/stresses resisting this strain, as determined by the initial elastic modulus of the matrix. In an elastic matrix, these forces are never relaxed, so that there is no remodeling of the matrix microenvironment. In a viscoelastic matrix, forces in the matrix can be relaxed over time as a result of mechanical yielding and remodeling of the matrix. The rate of stress relaxation determines the degree of this mechanical remodeling of the matrix. In fast-relaxing matrices, this facilitates adhesion-ligand clustering, cell shape change, proliferation and bone matrix formation by MSCs undergoing osteogenic differentiation.